

Expanding tubular microvessels on stiff substrates with endothelial cells and pericytes from the same adult tissue

Journal of Tissue Engineering
Volume 13: 1–17
© The Author(s) 2022
Article reuse guidelines:
sagepub.com/journals-permissions
DOI: 10.1177/20417314221125310
journals.sagepub.com/home/tej



Xiuyue Song^{1,2}, Yali Yu^{1,2}, Yu Leng^{1,2}, Lei Ma^{1,2,3}, Jie Mu^{1,4},
Zihan Wang¹, Yalan Xu^{1,2}, Hai Zhu⁵, Xuefeng Qiu⁶, Peifeng Li¹,
Jing Li¹ and Dong Wang^{1,3} 

Abstract

Endothelial cells (ECs) usually form a monolayer on two-dimensional (2D) stiff substrates and a tubular structure with soft hydrogels. The coculture models using ECs and pericytes derived from different adult tissues or pluripotent stem cells cannot mimic tissue-specific microvessels due to vascular heterogeneity. Our study established a method for expanding tubular microvessels on 2D stiff substrates with ECs and pericytes from the same adult tissue. We isolated microvessels from adult rat subcutaneous soft connective tissue and cultured them in the custom-made tubular microvascular growth medium on 2D stiff substrates (TGM2D). TGM2D promoted adult microvessel growth for at least 4 weeks and maintained a tubular morphology, contrary to the EC monolayer in the commercial medium EGM2MV. Transcriptomic analysis showed that TGM2D upregulated angiogenesis and vascular morphogenesis while suppressing oxidation and lipid metabolic pathways. Our method can be applied to other organs for expanding organ-specific microvessels for tissue engineering.

Keywords

Microvessel, endothelial cell, pericyte, culture medium, vascular heterogeneity

Date received: 20 April 2022; accepted: 25 August 2022

Introduction

Microvessels play essential roles in maintaining normal organ functions. Microvascular dysregulation happens in various diseases, such as fibrosis, tumor, and diabetic microvasculopathy.¹ Microvascular structural stability and proper function rely on microvascular endothelial cells (ECs) and pericytes.² Although many studies have focused on embryonic microvascular development using animal models, *in vitro* culture models of adult microvessels will provide more insights into the mechanisms of microvascular diseases in adulthood. The isolation and growth of microvessels from adult tissues can provide a platform for research on patient-specific diseases and benefit the development of precision medicine. The culture of adult microvessels will also promote the development of microvascular engineering *in vitro*.

There have been various *in vitro* culture models for adult microvessels.³ Active angiogenesis can be induced in

¹Institute for Translational Medicine, The Affiliated Hospital of Qingdao University, Medical College, Qingdao University, Qingdao, China

²School of Basic Medicine, Qingdao University, Qingdao, China

³Key Laboratory of Birth Regulation and Control Technology of National Health Commission of China, Shandong Provincial Maternal and Child Health Care Hospital, Jinan, China

⁴School of Pharmacy, Medical College, and Institute for Chemical Biology & Biosensing, College of Life Sciences, Qingdao University, Qingdao, China

⁵Department of Urology, Qingdao Municipal Hospital Affiliated to Qingdao University, Qingdao, China

⁶Department of Cardiovascular Surgery, Union Hospital, Tongji Medical College, Huazhong University of Science and Technology, Wuhan, China

Corresponding author:

Dong Wang, Institute for Translational Medicine, The Affiliated Hospital of Qingdao University, Medical College, Qingdao University, 38 Dengzhou Road, Qingdao, 266021, China.
Email: dongwang@qdu.edu.cn



tissue explant culture models, such as retina and aorta ring explants in a three-dimensional (3D) matrix,³ however, these models face challenges while being translated into clinical settings. It has been widely used to culture a pure population of primary ECs in most laboratories. The human umbilical vein is a popular source for primary EC isolation. ECs can also be isolated from other organs, for example, the kidney, then purified by flow cytometric sorting.^{4,5} The coculture models of ECs and pericytes have been developed to investigate the mechanisms of pericyte recruitment. The pericytes used in these experiments were usually isolated from the brain, an organ rich in pericytes.⁶ In recent years, pluripotent stem cells (PSCs) have been an emerging source for producing ECs, pericytes, and smooth muscle cells.⁷ However, it is a challenge for the vascular cells derived from PSCs to reflect the biological characteristics of a specific tissue or organ. Due to the heterogeneity of blood vessels throughout the body,⁸ the ideal culture models for adult microvessels would contain microvascular ECs and pericytes from the same adult tissue, which will benefit organ-specific studies.

In traditional methods, ECs are usually cultured in commercially available media and form a monolayer on the rigid surface of plastic dishes.³ Many efforts have been made to achieve a tubular morphology of microvessels *in vitro* to recapitulate the microvascular environment *in vivo*. ECs can form a network of tubular microvessels on the surface of a soft hydrogel, for example, Matrigel, which, however, can only be maintained for a few days.³ Tubular microvessels can also be obtained by 3D culture of ECs inside hydrogels, such as collagen, fibrin, Matrigel, and synthetic hydrogels.^{3,9} In recent years, micro-technologies, such as microfluidics, 3D printing, and ice templating,⁹ make it possible to fabricate elegant microvascular models. ECs can be seeded into the microchannels made by extracellular protein hydrogels and adhered to the channel walls to form a tubular vessel.¹⁰ ECs embedded in 3D hydrogels can self-assemble to form microvessels, and form a perfused microvascular network in microfluidic channels.¹¹ These microvessels in 3D hydrogels were usually maintained *in vitro* for 2 weeks. Although superior to 2D culture in forming tubular microvessels, 3D cultures face difficulties in characterizing the microvessels by conventional biochemical methods, such as immunostaining and confocal imaging. In addition, hydrogels are expensive for most laboratories.

In this proof-of-concept study, we aimed to establish a culture model for expanding adult tubular microvessels with the pericytes and ECs from the same tissue source on stiff regular plastic dishes. Microvessels were isolated from adult rats' subcutaneous soft connective tissue and cultured in the custom-made tubular microvascular growth medium on 2D stiff substrates (TGM2D). By activating Wnt/ β -catenin and inhibiting TGF β /Smad and ROCK activity, we successfully expanded tubular microvessels wrapped with the pericytes from the same tissue source of

ECs on regular plastic culture dishes. The tubular microvessels can be maintained for at least 4 weeks *in vitro*.

Materials and methods

Isolation of primary microvessels from adult rats

Male Sprague Dawley (SD) rats aged 8–10 weeks were euthanized by an overdose of isoflurane and bilateral thoracotomy. The subcutaneous soft connective tissue was harvested in an aseptic environment. The tissue pieces were digested in an enzymatic solution containing 2 mg/ml collagenase I (Worthington, Cat#LS004196), 5 mg/ml bovine serum albumin (BSA, Sigma, Cat#A1933), and 5 μ M Y27632 (Selleck, Cat#S1049) in DMEM (Invitrogen, Cat#12800017).

The cyclic digestion method was used to harvest primary microvessels. Every 10 min, the cell suspension was harvested, a new enzymatic solution was added to the remaining tissue, and the digestion cycle continued until all the tissue pieces were digested. The cell suspension was centrifuged at 1000 rpm for 4 min, and cell pellets were resuspended in phosphate-buffered saline (PBS). All the cell pellets were pooled together and filtered through a 30 μ m strainer to remove red blood cells and single cells. The long microvessel segments were collected from the strainer mesh and used for culture.

Culture of primary microvessels

The primary microvessel segments were cultured in regular plastic dishes and plates in different media. EGM2MV medium was purchased from Lonza (Cat# CC-3202). Our custom-made medium was DMEM/F12 (Invitrogen, Cat# 12400024), supplemented mainly with 2% fetal bovine serum (FBS, Gibco, Cat#10091148), 100 U/ml penicillin and 100 μ g/ml streptomycin (Gibco, Cat#15140122), 5 mM nicotinamide (Sigma, Cat#N0636), 1 mM (N-Acetyl-L-cysteine) NAC (Sigma, Cat#A9165), 50 μ M Vitamin C (Sigma, Cat#A4403), 3 μ M glutathione (Sigma, Cat#G6013), 10 μ g/ml insulin (Aladdin, Cat#I113907), 7.5 μ g/ml transferrin (Sigma, Cat#T0665), 40 nM Sodium Selenite (Sigma, Cat#S9133).

TGM2D was supplemented with 2 μ M Chir99021 (Selleck, Cat#S2924), 0.2 μ M A83-01 (Tocris, Cat#2939), 5 μ M Y27632 (Selleck, Cat#S1049), and 10 ng/ml VEGF (Peprotech, Cat#100-20). For the titration of A83-01, the concentrations included 0, 0.1, 0.2, 0.5, 1, and 2 μ M.

The cells were cultured in an incubator at 37°C, with 5% CO₂ and 95% humidity. The medium was changed every other day in the first 4 days and every day after that.

Total RNA extraction

Total RNA was extracted from the microvascular cells using Trizol (Invitrogen, Cat#15596026) according to the

manufacture instruction. The cells of a 60 mm dish were homogenized in 1 ml Trizol, centrifuged at $12,000\times g$ for 5 min at 4°C , and then the supernatant was transferred into a tube with 0.3 ml chloroform/isoamyl alcohol (24:1). The mixture was centrifuged at $12,000\times g$ for 10 min at 4°C , the upper aqueous RNA layer was transferred into a new tube with equal volume of isopropyl alcohol, and then centrifuged at $12,000\times g$ for 20 min at 4°C . The RNA pellet was washed with 1 ml 75% ethanol, and then centrifuged at $12,000\times g$ for 3 min at 4°C . The pellet was dried in air for 5–10 min. Finally, 50 μl DEPC water was added to dissolve the RNA, which was qualified and quantified using a Nano Drop and Agilent 2100 bioanalyzer (ThermoFisher).

mRNA library construction

The mRNA was purified by Oligo(dT)-attached magnetic beads and fragmented into small pieces. First-strand cDNA was generated by random hexamer-primed reverse transcription and a second-strand cDNA synthesis. A-Tailing Mix and RNA Index Adapters were added. The cDNA fragments were amplified by PCR, and then purified by Ampure XP Beads and dissolved in EB solution. The product was validated on an Agilent Tech 2100 bioanalyzer. The double stranded PCR products were denatured and circularized by the splint oligo sequence to make the final library, which was amplified with phi29 to make DNA nanoball with more than 300 copies of one molecular, which were loaded into the patterned nanoarray and pair end 150 bases reads were generated on DNBSEQ-T7 platform.

Sequencing analysis

The sequencing data was filtered with SOAPnuke (v1.5.2). The clean reads were mapped to the reference genome using HISAT2 (v2.0.4). Bowtie2 (v2.2.5) was applied to align the clean reads to the reference coding gene set then expression level of gene was calculated by StringTie (v2.1.2). KEGG and GO analysis were performed in DAVID Bioinformatics Resources (<https://david.ncifcrf.gov>). The heatmap and bubble plot were drawn by SRplot (<http://www.bioinformatics.com.cn>) according to the gene expression in different samples.

Quantitative RT-PCR analysis

Total RNA was extracted from the microvascular cells using Trizol (Invitrogen, Cat#15596026) according to the manufacture instruction. RNA quality was checked by measuring the optical density ratio at 260/280 nm on a nanodrop. RNA from each sample was reverse transcribed into cDNA by an Evo M-MLV RT Mix Kit (Accurate Biotechnology, Cat#AG11728). Experiment was carried out using the forward and reverse primers listed below.

Fold change in mRNA expression levels was calculated by the comparative Ct method, using the formula $2^{-(\Delta\Delta\text{Ct})}$ and GAPDH as a calibrator. The primer list:

Apln (AAGCCCAGAACTTCGAGGAC;GGCAGCATATTTCCGCTTCTG), Dll4 (AGTGTACTCCCGCACTAGCC;CGATGCCTCGGTAGGTAATCC), Kcne3 (ACAGATCGCAGAGTCAGATCAC;TGATTGTCTGGCCCTGTTCC), Pcdh12 (CAGCAGGTCTGAAGTGGGAG;GTAGCATCGTGCTTACCGGA), Plxnd1 (ATCGCCCAGGCCTTCATAGAT;TCTTCCGGTACTCGGGGAT), Car2, (GCTGGAATGTGTGACCTGGA;CCCAGCTGCAGGGTCATTTT), Wnt5a (TGGGCA CATTTCACGCTAT;TGTCCCTTGAGAAAGTCCC GC), Fzd1 (GCCTCACAACCAGTCCACAA;TGCTTTACAAATGCCACTCGG), Cxcl12 (AGCCTTAAACAAGAGGCTCAG;TGAGGGGTGGATCTCGCTCTT), Mmp9 (GGATCCCCAACCTTTACCAG;AAGGTCAGAACCGACCCTACA).

Immunostaining

The cells were fixed in 4% paraformaldehyde (PFA) for 30 min, washed with PBS for three times, permeabilized by 0.1% Triton for 10 min, blocked in 5% normal donkey serum for an hour, and incubated with primary antibodies in the blocking solution at room temperature. After 2 h of primary antibody incubation, the cells were washed in PBS for three times and incubated with secondary antibodies in blocking solution for 1 h at room temperature. The primary antibodies used in this study included CD31 (Abcam, Cat#ab28364; Santa Cruz, Cat#SC376764; Novus, Cat#AF3628), vWF (Proteintech, Cat#11778-1-AP), LYVE1 (Affinity, Cat#AF4202), NG2 (Proteintech, Cat#55027-1-AP), ZO1 (Proteintech, Cat#21773-1-AP), PDGFR β (Proteintech, Cat#13449-1-AP), CD45 (Proteintech, Cat#20103-1-AP), and SMA (Santa Cruz, Cat#sc-32251). The secondary antibodies used in this study were purchased from Invitrogen (Cat#A10040, A-21202, A-21447). Cell nuclei were stained by DAPI (4',6-diamidino-2-phenylindole). Confocal imaging was performed on a Leica SP8 confocal microscope.

Flow cytometry

The primary microvessels were cultured in TGM2D medium for 3 or 7 days before flow cytometric analysis. For flow cytometry, the primary microvessels were dissociated into single cells by accutase (Sigma, Cat#A6964). The staining procedure was performed on ice, including the following: blocking in 3% normal donkey serum for 15 min, incubation in primary antibodies (CD31 from Novus, Cat#AF3628, NG2 from Proteintech, Cat#55027-1-AP, CD45 from Proteintech, Cat#20103-1-AP), secondary antibodies (Invitrogen, Molecular probes, Cat#A10040, A-21202, A-21447). The cells were suspended in the sorting buffer containing 1% BSA and 1 mM EDTA in PBS, went through a single-cell strainer before analysis on a Beckman CytoFLEX LX cytometer.

Statistical analysis

To quantify the features of the microvessels, at least three images randomly selected from each group were analyzed using ImageJ. The total microvessel length and branch point numbers used for analysis were the sums on a $10\times$ image area. Data were presented as means \pm SD unless otherwise indicated. One-way or two way ANOVA was performed on the data of multiple groups, followed by Bonferroni post hoc tests. Student's *t*-test was used to analyze the differences between two groups.

Results

Expanding tubular adult microvessels in TGM2D

Primary microvessels were isolated from adult SD rats (Figure 1(a)). The subcutaneous soft connective tissue was harvested from adult rats and digested in an enzymatic solution containing mainly collagenase I at 37°C. We designed a cyclic digestion method to improve the viability of primary microvessels (Figure 1(a)). Every 10 min, we harvested cell suspension from the digestion tube and added a freshly prepared enzymatic solution to the tube. The cell suspension was centrifuged, and the pellets were re-suspended in a collection tube containing phosphate-buffered saline (PBS). The digestion cycle continued until all the tissue pieces were wholly digested. The cell suspensions were pooled together and filtered through a 30 μ m strainer to remove red blood cells and other single cells. The microvessel segments were collected from the strainer mesh (Figure 1(a)). We obtained the microvessel segments with a length range of about 50–150 μ m (Figure 1(b); Supplemental Figure S1). In the commercially available medium, EGM2MV, ECs formed a monolayer on the rigid surface of plastic culture dishes, consistent with traditional culture methods (Figure 1(c)).

To make a better culture system, we set up to formulate a basal medium that was DMEM/F12 supplemented with some ingredients. Considering that oxidative stress was the primary threat to the cells *in vitro*, we tested the effect of adding several antioxidants, such as nicotinamide, NAC, glutathione, and Vitamins C, to the DMEM/F12 medium (See Materials and methods). We then screened signaling pathways that may impact the growth of adult microvessels *in vitro*. Vascular endothelial growth factor (VEGF) was not added in this screening because its potent proangiogenic effect may mask any roles of other signaling pathways. During 2 weeks of culture *in vitro*, most groups' culture dishes were covered by lipid-like cells characterized by the accumulation of lipid-like droplets, except those supplemented with Chir99021 (C) (Figure 1(d)). Chir99021 is a GSK3 β inhibitor and thus stabilizes β -catenin and activates the canonical Wnt signaling pathway. This result was consistent with a previous report that

upregulated Wnt signaling inhibited adipogenesis.¹² Thus, Chir99021 was added to the basal medium for the following study.

ECs may undergo endothelial-to-mesenchymal transition and lose EC identity, during which the TGF β signaling pathway is a master regulator.¹³ We thus examined the effect of an inhibitor of the TGF β /Smad signaling pathway, A83-01 (A), in combination with Chir99021. We further examined another small molecule, Y27632 (Y), a ROCK inhibitor that was reported to improve embryonic stem cell survival *in vitro*.¹⁴ The different combinations of these three small molecules were investigated (Figure 1(e)). The primary microvessels were cultured for about a week and analyzed by immunofluorescence staining. We found that the combination of the three small molecules, C+A+Y, significantly promoted the growth of tubular microvessels (Figure 1(e) and (f)). The addition of VEGF further significantly increased microvessel length and branch point number (Figure 1(e) and (f)). We referred to the medium containing C, A, Y, and VEGF as TGM2D, which significantly promoted the growth of adult tubular microvessels *in vitro*, compared to the commercially available medium EGM2MV (Figure 1(g)).

TGM2D upregulated angiogenesis and downregulated oxidation and lipid metabolism

We performed mRNA sequencing to analyze gene expression profiles of the microvessels in TGM2D (T) and EGM2MV (E) compared to fresh primary microvessels (V). We focused on the genes up- or down-regulated in EGM2MV and TGM2D (Supplemental Figure S2, A). KEGG pathway analysis showed that EGM2MV specifically upregulated the pathways of oxidation and lipid metabolism (Supplemental Figure S2, B). GO analysis showed that the elevated biological processes in EGM2MV included mainly oxidation, lipid metabolism, and aging, which involved increased mitochondrial activities (Figure 2(a); Supplemental Figure S2, C). On the contrary, oxidation- and lipid metabolism-related processes were significantly suppressed in TGM2D (Supplemental Figure S2, A). TGM2D specifically upregulated Notch, TNF, Rap1, Ras, PI3K-Akt, and chemokine signaling pathways, which were closely related to angiogenesis (Supplemental Figure S2, B). GO analysis showed that the upregulated biological processes in TGM2D included mainly angiogenesis, vascular branch formation, vascular remodeling, EC proliferation, and migration, which mainly involved cell-cell junctions between ECs, contributing to the structural integrity of microvessels (Figure 2(b); Supplemental Figure S2, D).

The genes for the identity of ECs (Cd31, Cdh5, Tie1^{15,16}) and endothelial progenitor cells (Cd34, Kdr, and Kit)¹⁷ were down-regulated in EGM2MV but significantly upregulated in TGM2D (Figure 2(c)). Sox family members, including Sox7, 17, and 18, were also upregulated in

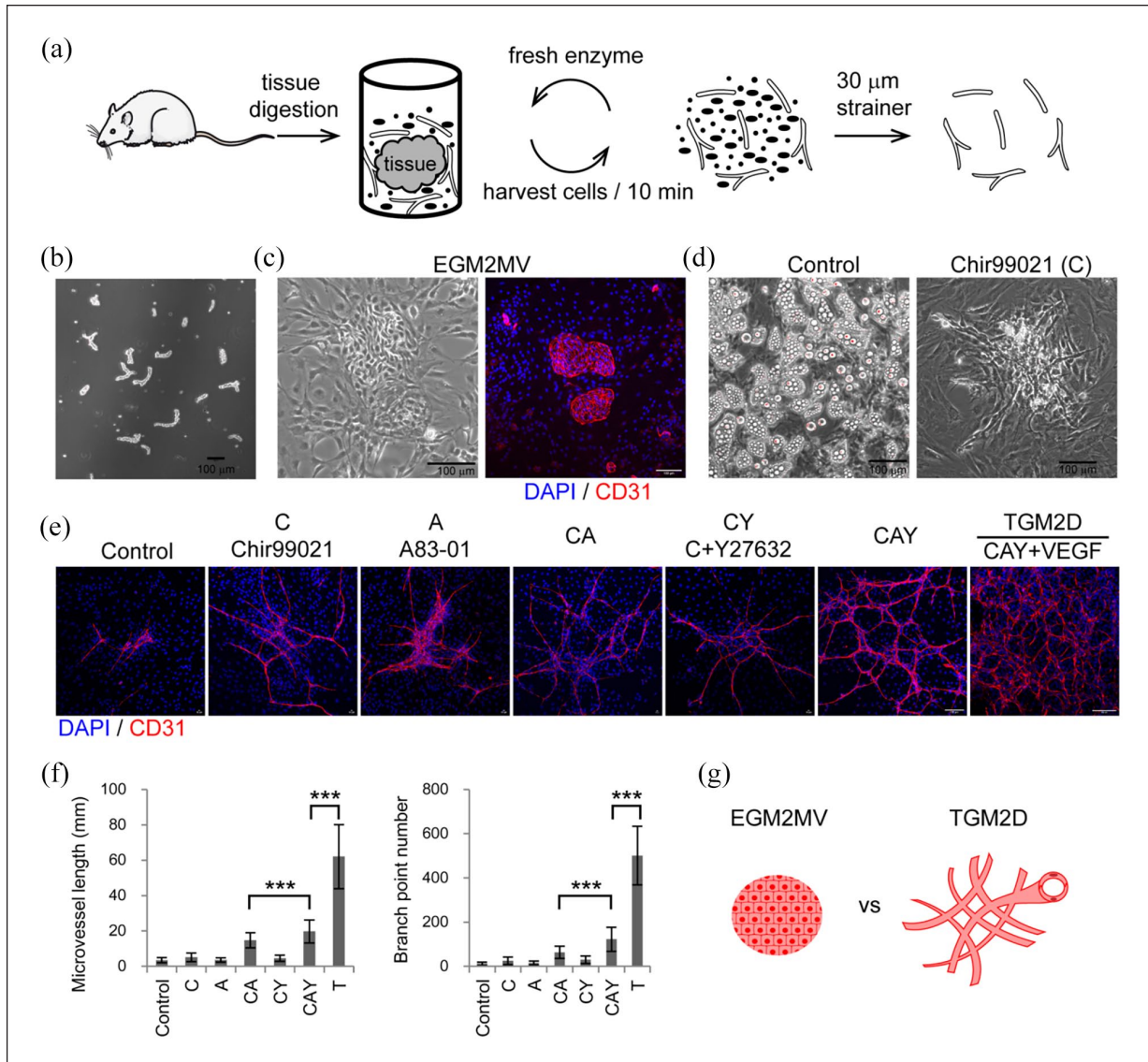


Figure 1. Expand adult tubular microvessels in vitro: (a) the procedure of isolating microvessels from adult SD rats' subcutaneous soft connective tissues by cyclic enzymatic digestion, (b) phase contrast image of primary microvessels, (c) phase contrast and immunofluorescence images of the microvessels cultured in EGM2MV medium, (d) phase-contrast images of the primary microvessels cultured in the media of control and Chir99021, (e) immunofluorescence images of primary microvessels cultured in different media, (f) quantification of the microvessels in different experimental groups including control ($n=81$), C ($n=84$), A ($n=72$), CA ($n=97$), CY ($n=58$), CAY ($n=61$), and TGM2D (CAY + VEGF) ($n=9$). Data were presented as mean \pm SD. One-way ANOVA was performed on the data, followed by Bonferroni post hoc tests. *** $p < 0.001$, and (g) illustration of the morphologies of microvessels cultured in EGM2MV and TGM2D. The antibody against CD31 was used to label endothelial cells. DAPI was used to label cell nuclei. Scale bars, 100 μ m.

TGM2D for the differentiation and maturation of ECs.¹⁸ TGM2D also upregulated the expression of *Apln*, which was recently reported to mark an EC subpopulation contributing to vascular development^{19,20} and regeneration.^{21,22} Proangiogenic genes were significantly upregulated in TGM2D, such as *Mmp9*,²³ *Angpt2*,²⁴ *Wnt* signaling genes (*Wnt4*, *Wnt5a*, *Cpz*, *Sfrp2*),²⁵ and *Notch* signaling genes (*Notch1*, *Notch3*, *Dll4*, *Jag1*, *Hey1*),^{26–28} and chemokine signaling (*Cxcl12*, *Cxcr4*, and *Ackr3*)^{29,30} (Figure 2(c) and (d)). Genes significantly upregulated in TGM2D also

included: *Kcne3*,³¹ *Esm1*,³² as tip EC markers; *Car2*, which promoted EC survival,³³ *Pcdh12*, a protocadherin,³⁴ *Plxnd1*, for EC mechanotransduction.³⁵

In addition to the markers of ECs, TGM2D also upregulated *Pdgfrb* and *Pdgfrb*, which were expressed in ECs and pericytes respectively for pericyte recruitment.³⁶ Other pericyte markers, including *Mcam* (Cd146) and *Cspg4* (Ng2)³⁷ were also upregulated in TGM2D. These results indicated that both ECs and pericytes of the same microvessel segments were expanded in TGM2D.

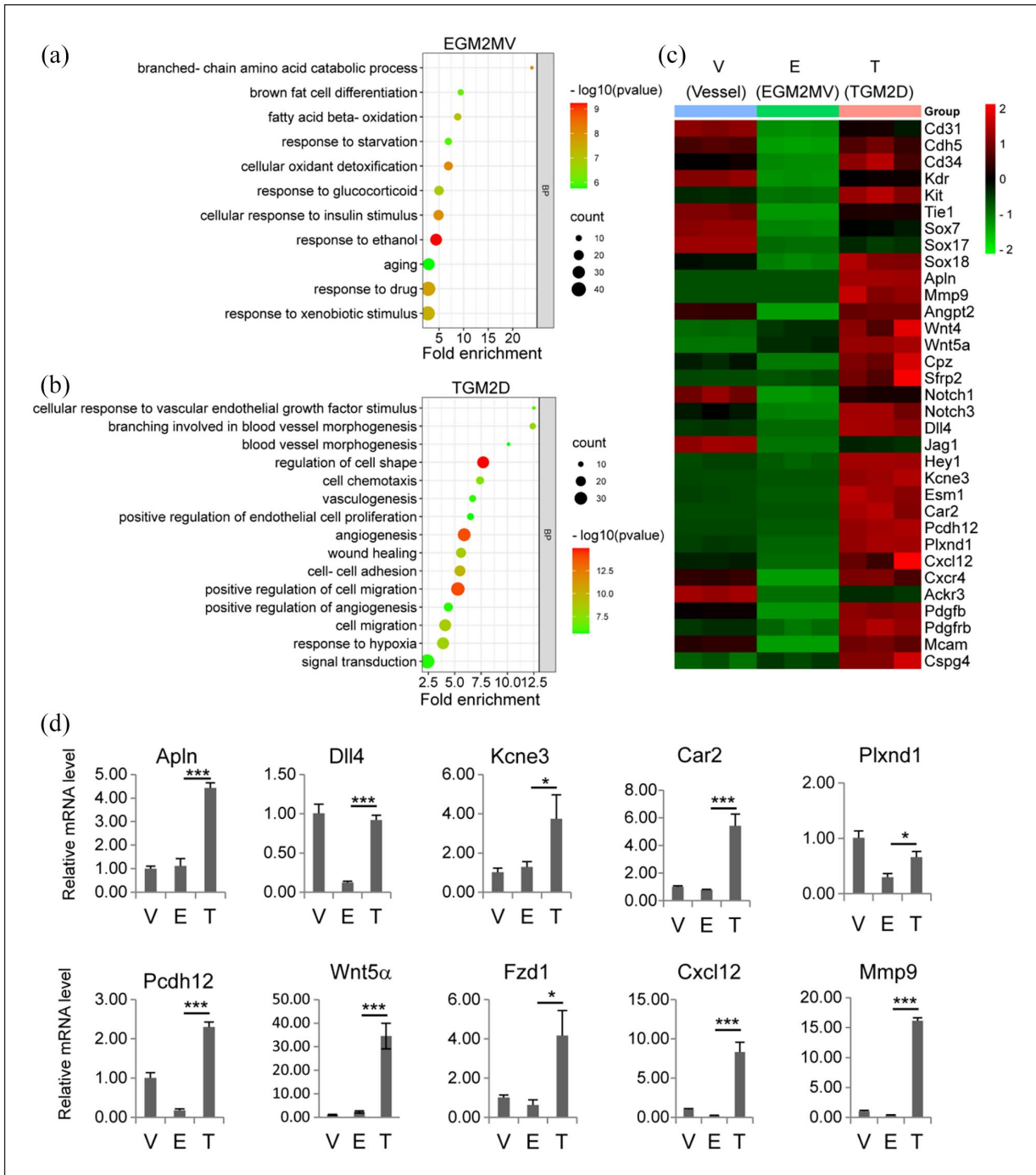


Figure 2. Transcriptomic analysis of TGM2D: (a and b) GO analysis of the biological processes upregulated in EGM2MV (a) and TGM2D (b), (c) the heatmap of the genes that were downregulated in EGM2MV and upregulated in TGM2D and (d) quantitative RT-PCR verification of gene expression in different groups. Data were presented as mean \pm SD. One-way ANOVA was performed on the data, followed by Bonferroni post hoc tests. * $p < 0.05$, *** $p < 0.001$.

Individual roles of Chir99021, Y27632, and A83-01 in tubular microvessel growth *in vitro*

To investigate the roles of the small molecules in TGM2D, VEGF was supplemented to the basal medium to obtain enough microvessels for analysis. The primary microvessels

were cultured in different groups of the combinations of the three small molecules. During a week of culture *in vitro*, a single small molecule Chir99021 alone was enough to promote tubular microvessels' growth significantly. Adding Y27632 further increased microvessel length and branch point number. Adding A83-01 to C or CY groups did not

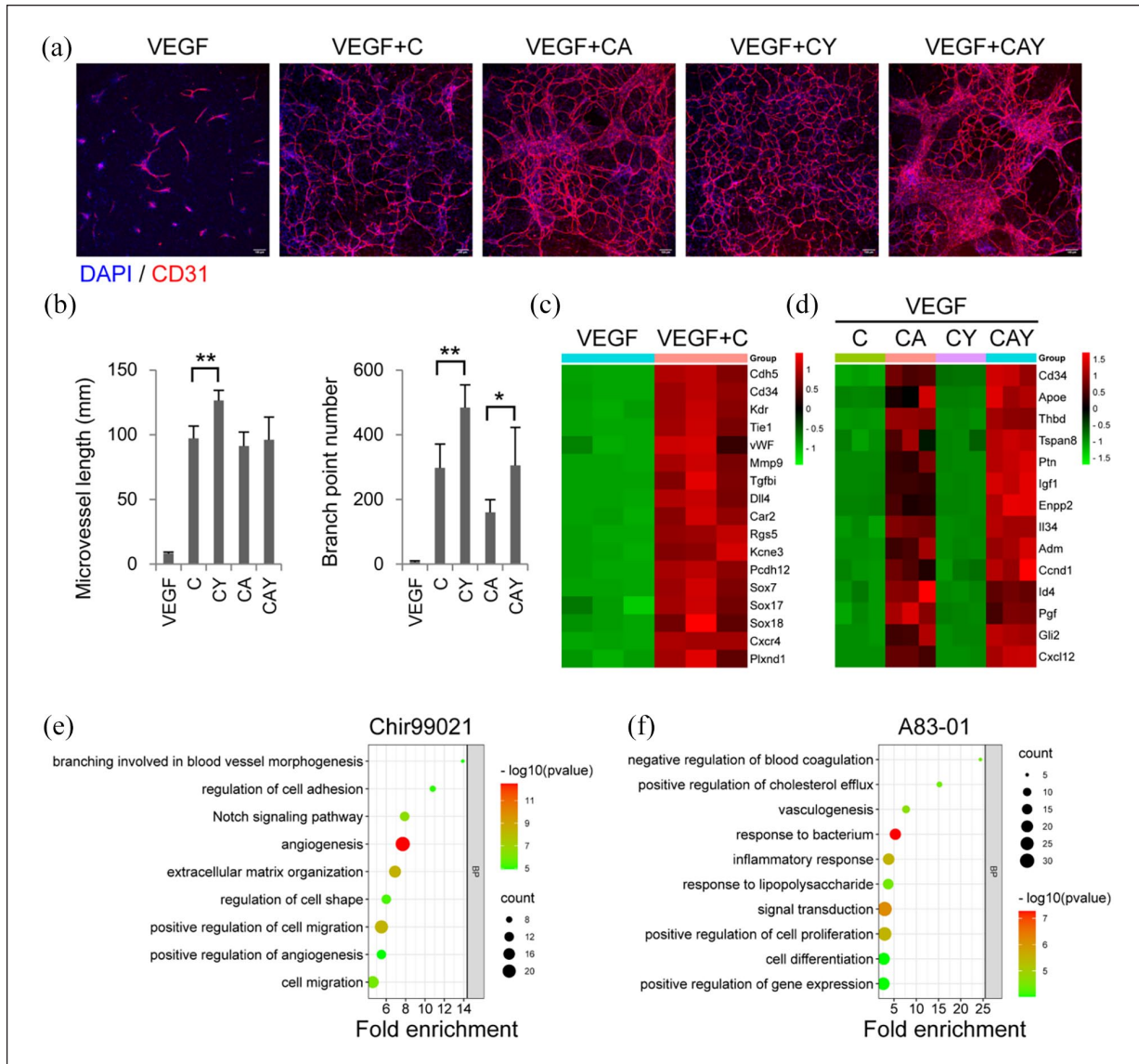


Figure 3. The roles of individual small molecules: (a) immunofluorescence images of the microvessels in different groups. The antibody against CD31 was used to label endothelial cells. DAPI was used to label cell nuclei. Scale bars, 100 μ m. (b) quantification of microvessel length and branch point number in different groups (*n* = 6). Data were presented as mean \pm SD. One-way ANOVA was performed on the data, followed by Bonferroni post hoc tests. **p* < 0.05, ***p* < 0.01. (c and d) the heatmaps of genes upregulated by Chir99021 (c) and A83-01 (d) in different groups, and (e and f) GO analysis of the biological processes upregulated by Chir99021 (e) and A83-01 (f).

benefit microvessel length or branch point number but produced some local areas with wide EC bundles (Figure 3(a) and (b)).

Transcriptomic analysis showed that the upregulated expression of most proangiogenic genes was mainly attributed to Chir99021, which acted as a Wnt agonist and induced the activation of the Notch signaling and other pathways associated with angiogenesis, branch formation, and cell migration (Figure 3(c) and (e)). A83-01 played a minor role in angiogenesis but contributed to preserved EC functions by upregulating the expression of genes related to

cholesterol efflux (Apoe), anti-coagulation (Thbd), and cell proliferation (such as Pgf, Igf1, and Adm.) (Figure 3(d) and (f)). Both Chir99021 and A83-01 promoted the expression of the progenitor marker CD34, indicating that EC progenitor properties were maintained and EndoMT was suppressed (Figure 3(d)). Interestingly, the addition of Y27632 did not significantly change the gene expression profiles of the microvessels (data not shown), although there was indeed an improvement in the microvascular length and branch formation (Figure 3(a) and (b)). Y27632 may only take effect at the protein level through regulating cell contractility.

Long-term culture of adult tubular microvessels *in vitro*

We next examined the long-term performance of the three small molecules in the growth of microvessels *in vitro*. For a total of 8 weeks of culture, the cells were fixed and immunostained for EC marker CD31 at different time points: 1, 2, 3, 4, and 8 weeks. Although Chir99021 significantly promoted the growth of microvessels during the first week (Figure 3), the microvessels in the Chir99021 medium degraded quickly from the second week (Figure 4(a), (e), and (f)). The addition of A83-01 to Chir99021 medium slightly rescued the microvessels from the second week (Figure 4(b), (e), and (f)). Y27632 had a noticeable effect on the survival of microvessels from the second week (Figure 4(c)–(f)). The full TGM2D, containing C, A, and Y, could sustain microvascular growth for 8 weeks (Figure 4(d)–(f)). Microvascular length and branch formation were relatively high for at least 4 weeks (Figure 4(d)–(f)). The wide EC bundles in the groups of CA and CAY disappeared, and all the ECs adopted a tubular structure from the second week, indicating that active microvascular remodeling happened during culture *in vitro* (Figure 4(b) and (d)).

Preserving syngeneic pericytes around tubular microvessels *in vitro*

There were few LYVE1⁺ lymphatic endothelial cells in the culture, indicating that our custom-made TGM2D could specifically expand tubular blood vessels (Figure 5(a)). The adult tubular microvessels also showed strong endothelial marker vWF (Figure 5(b)) and the tight junction protein ZO1 (Figure 5(c)). More importantly, plenty of pericytes around the microvessels expressed the markers including NG2, PDGFR β , and α SMA (Figure 5(d)–(f)).

The digestion procedure would give rise to microvessels and other types of cells, including adventitial cells, fibroblasts, and immune cells. Our method excluded most of these single cells by cell straining and obtained a relatively pure population of microvessel segments from the strainer mesh (Figure 1(b)). We performed flow cytometry and immunostaining analysis to examine whether there were immune cells in the culture (Figure 6).

We tried digesting the primary microvessels into single cells by incubating them in the enzymatic solution for a longer time, which led to cell death. In our hands, it was not easy to dissociate the primary microvessels into single cells during the first 2 days of culture. Thus, we performed flow cytometric and immunostaining analysis on the primary microvessels at 3 and 7 days. The results showed very few CD45⁺ cells in the microvascular culture (Figure 6(a) and (b)). There were about 10% of CD31⁺ ECs and 9% of NG2⁺ pericytes on day 3, which were around 4% and 20%, respectively, on day 7 (Figure 6(c)). By immunostaining,

we also found many NG2⁺ pericytes (Figure 6(d), arrow) and a few CD31⁺ ECs (Figure 6(d), arrowhead) expressing the proliferation marker Ki67 on day 7. These results suggest that pericytes actively proliferated *in vitro*, which may explain the lower percentage of ECs during culture. We also noticed some CD31[−]NG2[−]CD45[−] cells in the areas far from microvessels, which may be derived from pericyte differentiation or residual fibroblasts. We will evaluate the significance of these uncharacterized cells and investigate them in our future studies.

The balance between the ECs and pericytes

TGF β signaling pathway is essential for the differentiation and maturation of vascular mural cells, including smooth muscle cells and pericytes.³⁸ There were still some NG2⁺ pericytes around microvessels in a week of culture in TGM2D containing A83-01 (Figure 5). Thus, we investigated whether NG2⁺ pericytes still existed in a long-term culture of 2 weeks, when TGF β signaling was inhibited by different concentrations of A83-01. We found that higher concentrations of A83-01 induced a higher density of microvessels and the concentration of 0.5 μ M gave the maximal level of microvessel length and branch formation (Figure 7), which was consistent with previous report.³⁹ However, there were few NG2⁺ pericytes when A83-01 concentration was bigger than 0.2 μ M. (Figure 7). Restoration of the TGF β signaling by removing A83-01 from the medium at the second week rescued NG2⁺ pericytes to some extent (Figure 8). However, NG2⁺ pericytes cannot be recovered if A83-01 was removed at the third week (data not shown).

Discussion

This study presented a model platform for expanding tubular microvessels with the ECs and pericytes from the same tissue on the rigid surface of regular culture dishes. The subcutaneous soft connective tissue of the adult body contains microvessels, fibroblasts, and some stem cells.^{40–42} It can be relatively easily obtained during minor surgeries, such as liposuction, plastic surgeries, and foreskin surgeries, making it a promising source for translational medicine.^{43–47} In traditional EC isolation methods, the tissues were digested for a long time until single ECs were obtained. Long-term exposure to digestive enzymes may harm the cells to some extent. The isolated single ECs lost their microenvironment, including cell-cell connections between ECs and between ECs and pericytes. In this study, we developed a cyclic digestion method to maximize the viability of primary cells and the structural integrity of microvessels. This method can be applied to primary cell isolation from other tissues and organs in general.

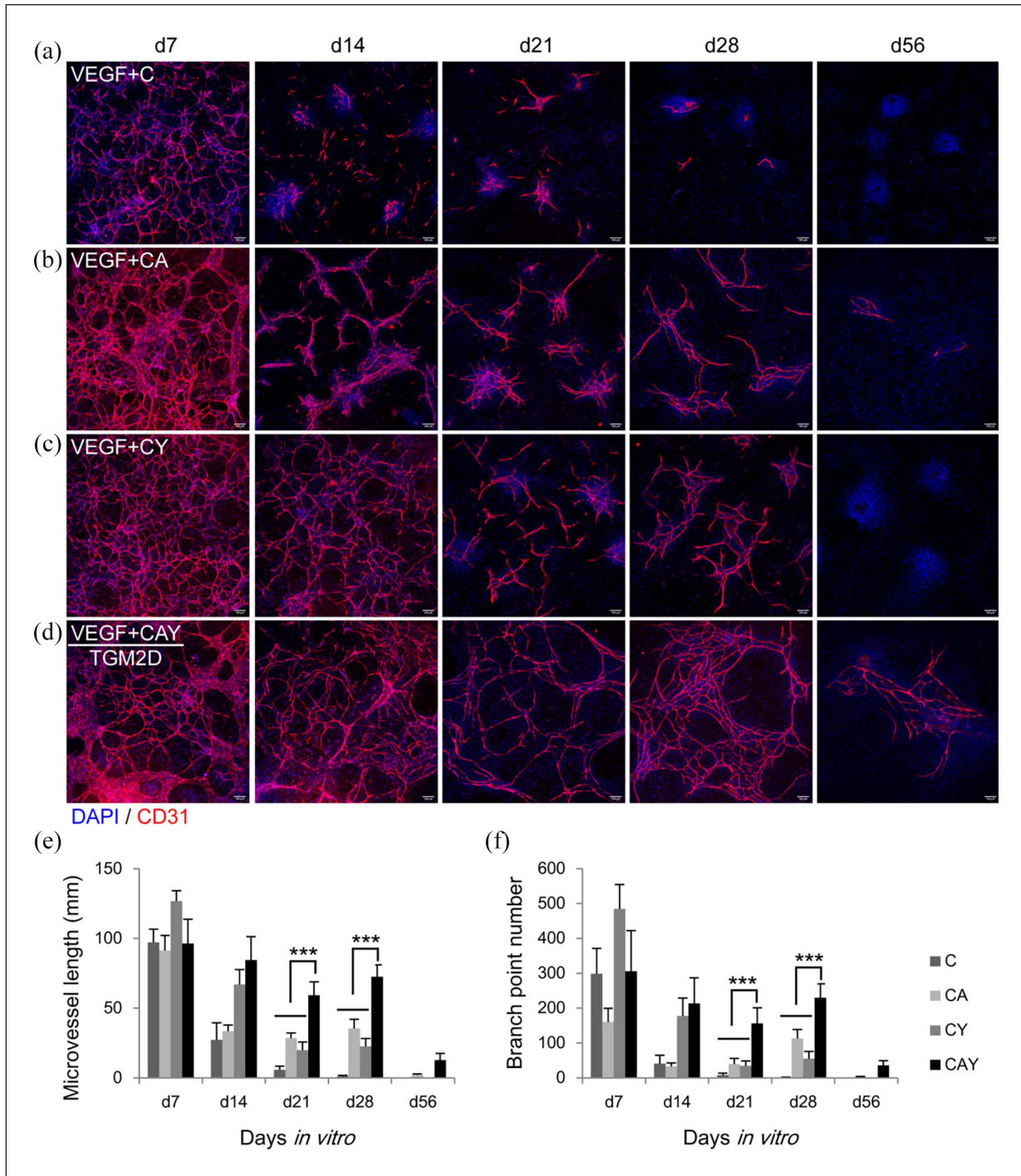


Figure 4. Time-lapse analysis of the microvessels in different media: (a–d) immunofluorescence images of the microvessels in the media supplemented with C (a) CA (b), CY (c), and CAY (d) in the presence of VEGF. The antibody against CD31 was used to label endothelial cells. DAPI was used to label cell nuclei. Scale bars, 100 μ m. (e and f) quantification of microvessel length and branch point number in different groups at different time points ($n=6$). Data were presented as mean \pm SD. Two-way ANOVA was performed on the data, followed by Bonferroni post hoc tests. *** $p < 0.001$.

The maintenance of tubular morphology of adult microvessels in this study was achieved through the orchestration of multiple pathways. One of the main threats to the cells cultured *in vitro* is oxidative stress, which induces DNA

damage, senescence, and apoptosis.⁴⁸ Oxidation was also a major biological process in the culture of EGM2MV (Figure 2(a)). The addition of antioxidants may contribute to the downregulation of oxidation pathways in TGM2D. The

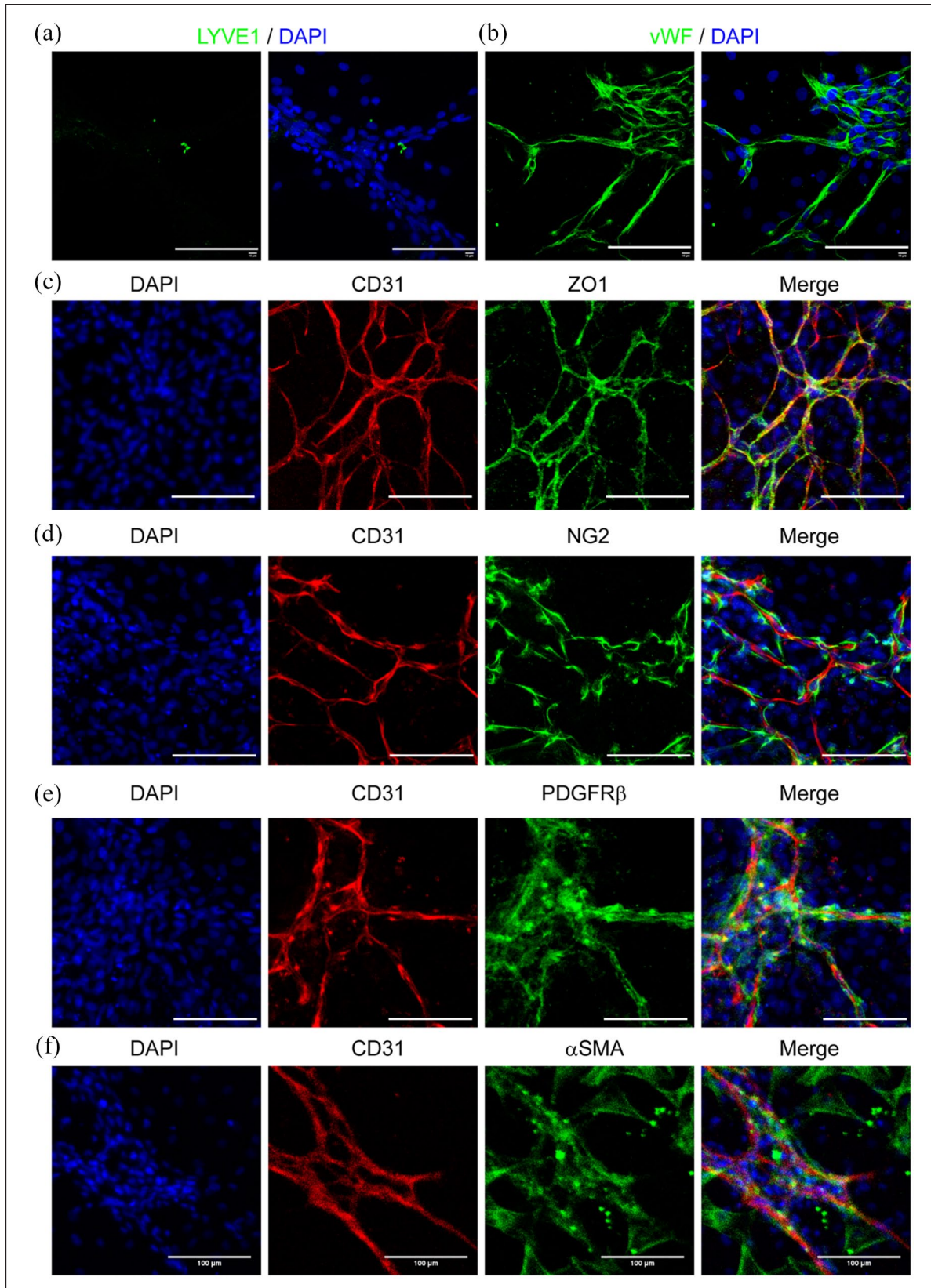


Figure 5. Endothelial and pericyte marker expression in TGM2D. The microvessels were cultured in TGM2D for 1 week and then immunostained by the antibodies against LYVE1 (a), vWF (b), CD31 (c–f), ZO1 (c), NG2 (d), PDGFR β (e), and α SMA (f). Nuclei were stained by DAPI. Scale bars, 100 μ m.

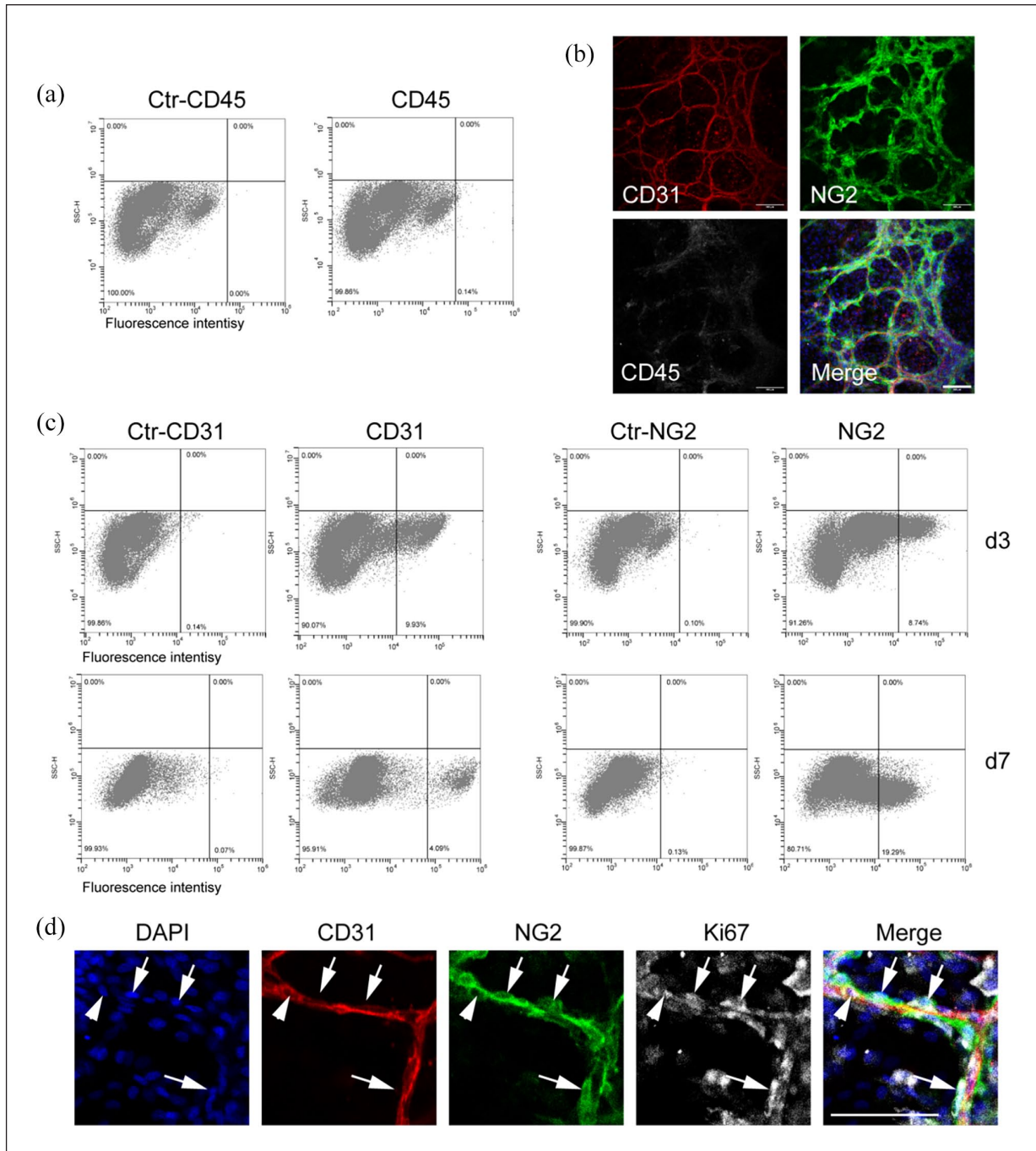


Figure 6. Flow cytometric analysis of primary microvessels: (a and c) the primary microvessels were cultured in the TGM2D medium for 3 (a and c) and 7 (c) days and analyzed by flow cytometry. Primary antibodies included CD31, NG2, and CD45. (b and d) the primary microvessels were cultured in the TGM2D medium for 7 days and immunostained by antibodies against CD31, NG2, CD45, and Ki67. DAPI stained nuclei. Scale bars, 100 μ m.

GSK3 β inhibitor Chir99021 upregulated Wnt signaling and played a dual role in the system. Activated Wnt signaling has been reported to suppress adipogenesis.¹² On the other hand, Wnt signaling was a master regulator in angiogenesis, blood vessel morphogenesis during embryonic development and

adult tissue regeneration.⁴⁹ Our results showed that the treatment of Chir99021 alone could activate most of the proangiogenic genes of adult microvessels (Figure 3(c) and (e)), indicating that Wnt signaling also played a central role in the tubular microvessel growth *in vitro*.

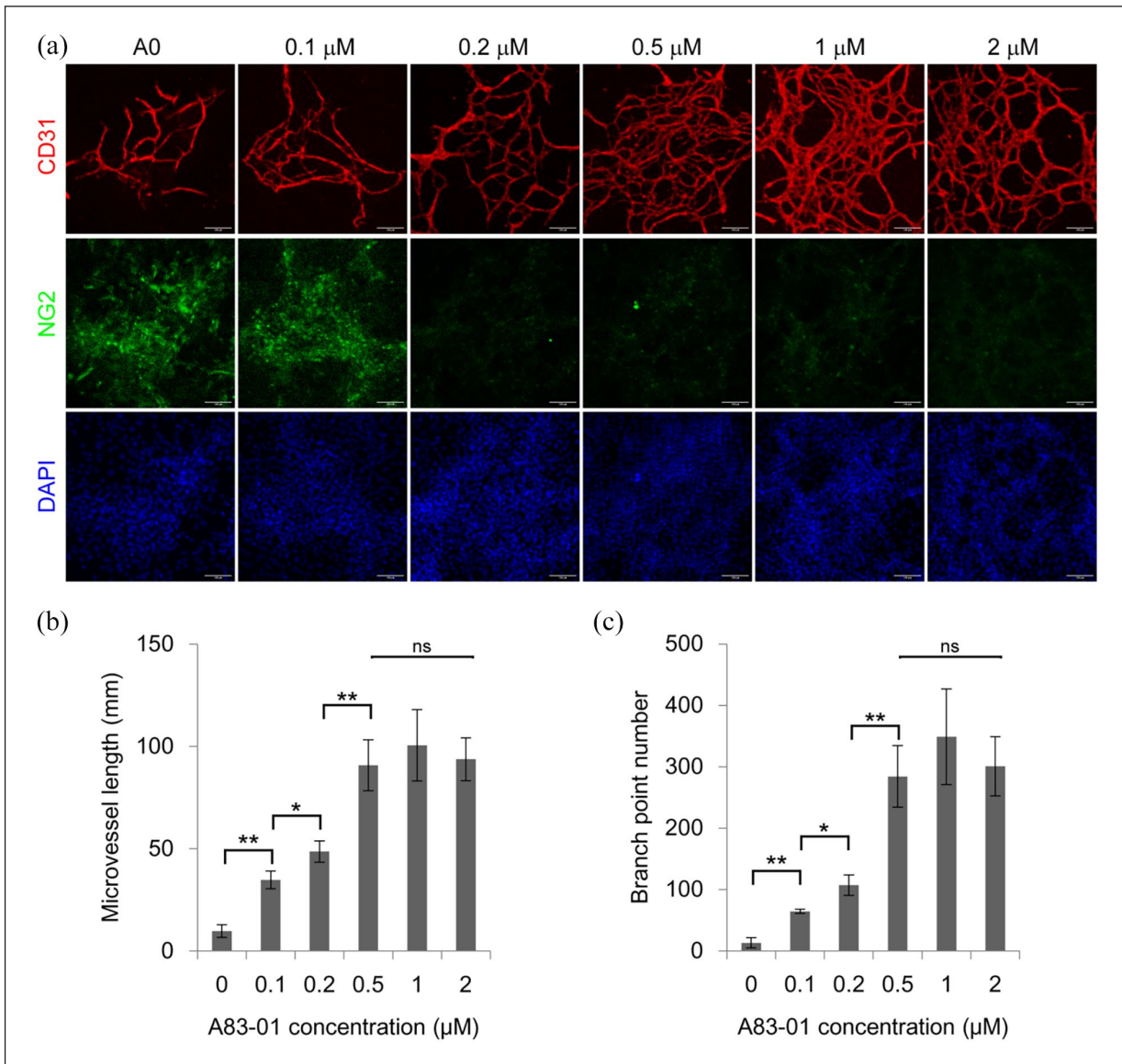


Figure 7. The effect of TGF β inhibitor A83-01 on microvessels: (a) the primary microvessels were cultured in the media supplemented with different concentrations of A83-01, including 0, 0.1, 0.2, 0.5, 1, 2 μM , for 2 weeks, and immunostained by the antibodies against CD31 and NG2. Nuclei were stained by DAPI. Scale bars, 100 μm . (b and c) quantification of microvessel length and branch point number in different groups. Data were presented as mean \pm SD. One-way ANOVA was performed on the data, followed by Bonferroni post hoc tests. * $p < 0.05$, ** $p < 0.01$.

TGF β signaling pathway is essential for vascular development as it modulates the differentiation and maturation of vascular mural cells, including smooth muscle cells⁵⁰ and pericytes.⁵¹ On the other hand, TGF β signaling can induce the loss of EC identity through endothelial-to-mesenchymal transition (EndoMT).¹³ TGF β inhibition maintained EC identity and proliferation.³⁹ Our results showed that the inhibition of TGF β signaling by A83-01 upregulated the expression Cd34, a marker for endothelial progenitor cells.⁵² Treatment of A83-01 also promoted the expression of the genes for EC proliferation, such as Pgf, Igf1, and Adm. More importantly, the critical functional

genes, such as Apoe for cholesterol transport and Thbd for anti-coagulation, were upregulated by the treatment of A83-01 (Figure 3). All these results indicate that the inhibition of TGF β /Smad signaling by A83-01 promoted EC proliferation and maintained EC functions.

Y27632 is a ROCK inhibitor that has been widely used in the culture of pluripotent stem cells and functions to promote cell survival *in vitro*.¹⁴ Studies in corneal endothelium showed that Y27632 promoted cell proliferation by upregulating Cyclin D and downregulating p27 gene expression.⁵³ However, few genes were influenced by the addition of Y27632 in our study (data not shown), indicating that

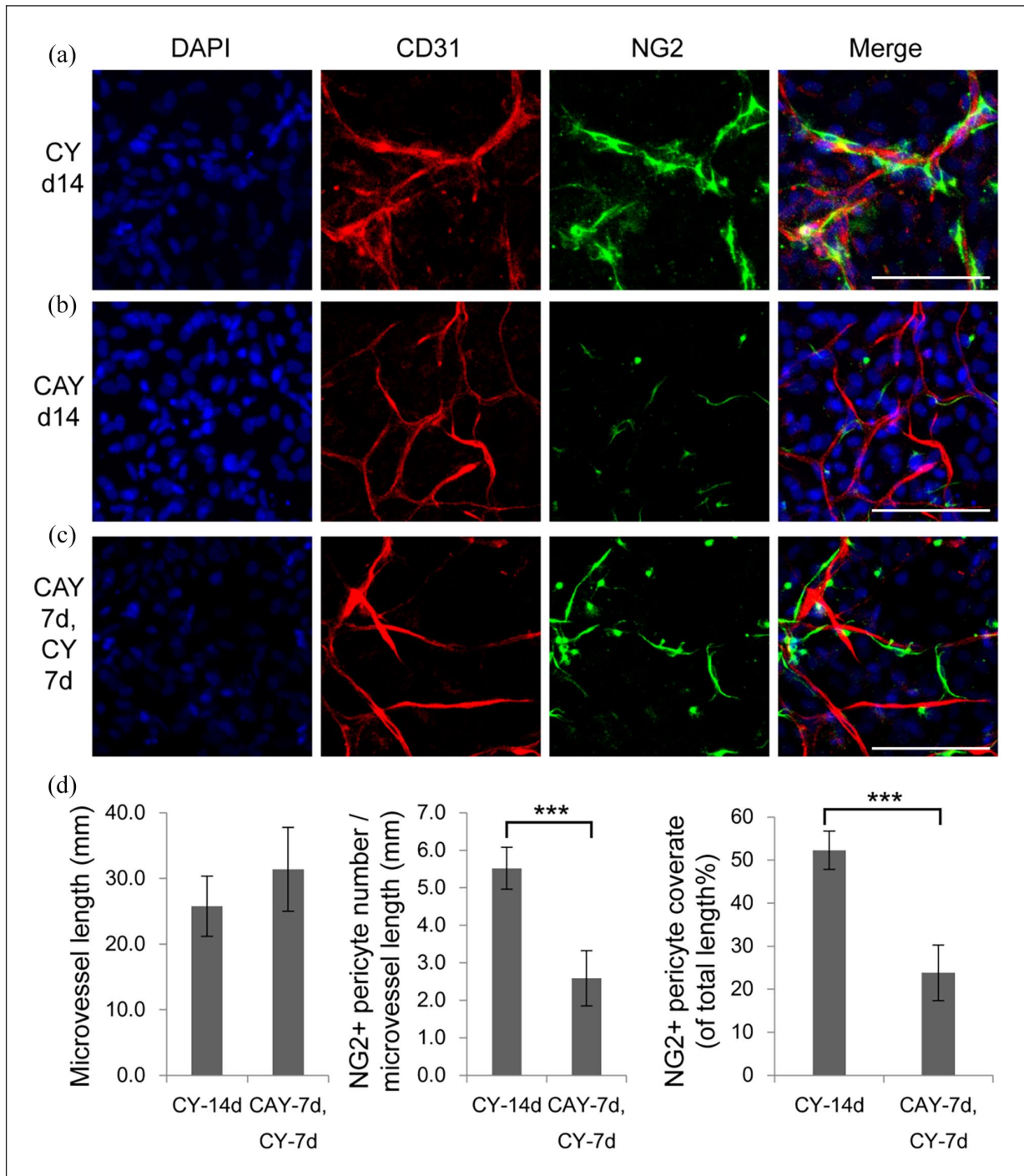


Figure 8. Dynamic regulation of NG2 pericytes by A83-01: (a–c) the primary microvessels were cultured in CY for 14 days (a), in CAY for 14 days (b), and in CAY for 7 days, followed by CY for another 7 days (c), then immunostained by antibodies against CD31 and NG2. Nuclei were stained by DAPI. Scale bars, 100 μ m. (d) quantification of microvessel length, NG2⁺ pericyte number per microvessel length, and NG2⁺ pericyte coverage ratio of total microvessel length (%). Data were presented as mean \pm SD. Student's t-test was performed to analyze significant differences between groups. *** $p < 0.001$.

Y27632 may take effect at the protein level. Y27632 has been reported to reduce cell contractility by down-regulating the phosphorylation of non-muscle myosin light chain II (MLC).⁵⁴ As pericytes wrap around microvessels and exert

contractile forces to the EC tubules and limit their growth,⁵⁵ Y27632 may promote microvascular tubule growth and branch formation by reducing the contractility of ECs and pericytes, which needs further investigation.

There have been several models for engineering tubular microvessels *in vitro*. A classic method is to culture ECs on the surface of Matrigel, and ECs will self-assemble into tubules and form a network, which, however, can only survive a few days.³ The ECs can also self-assemble into tubular structures inside a 3D matrix, such as collagen, Matrigel, and fibrin gels.³ Microfluidics techniques can make these 3D microvessels perfused, better-mimicking microvessels *in vivo*.³ These tubular microvessels in 3D hydrogels were usually maintained and investigated for up to 2 weeks.³

Most microvascular diseases are chronic diseases and take place in years or decades. The potential effect of a treatment may not emerge in a short time. A goal in the research of microvascular engineering is to maintain the culture of microvessels for a longer time. In this study, the microvessels in the experimental groups of C, CA, CY, and CAY had minor differences at the first week time point, but they behaved distinctly from the second to eighth week (Figure 4). The microvessels in group C quickly deteriorated in the second week, indicating that the activated Wnt signaling pathway alone promoted angiogenesis but was not enough to maintain the structural stability of microvessels *in vitro*. The beneficial effect of Y started to emerge from the second week. Adding Y to the media C or CA significantly improved microvessel length and branch formation. The addition of A to CY medium further promoted microvessel stability, possibly through upregulating the genes related to EC functions and proliferation (Figure 3). The microvessel length and branch formation in TGM2D (VEGF + CAY) were maintained at a relatively high level for at least 4 weeks *in vitro* (Figure 4). The time period of the third and fourth weeks had relative stable microvessels, which are a proper candidate for experimental manipulations (Figure 4).

There was a subtle balance between the ECs and pericytes in this model. Pericytes play a vital role in regulating microvessel structural stability and functions.³⁶ NG2 is a glycoprotein located on the plasma membrane of pericytes and regulates microvessel integrity.³⁶ Genetic knock-out studies showed that NG2^{-/-} animals had fewer microvessels than normal controls.⁵⁶ Our results are consistent with previous reports that TGF β signaling is essential for the differentiation and maturation of pericytes.³⁸ Although there were slight differences in NG2⁺ pericytes between CY and CAY media at the first week, a long-term culture of 2 weeks in CAY medium significantly reduced the number of NG2⁺ pericytes around microvessels (Figures 7 and 8). NG2⁺ pericytes can be preserved by removing A83-01 from the medium from the second week (Figure 8), but they will vanish if A83-01 was removed from the third week. These results indicate that the maintenance of NG2⁺ pericytes requires TGF β signaling. On the other hand, TGF β signaling played an opposite role in ECs. TGF β inhibition was required to for maintaining EC identity and functions *in vitro*.^{13,39} Future studies are warranted to

investigate how to coordinate the growth of syngeneic ECs and pericytes in tubular microvessels *in vitro*.

Our method will have broad applications in microvascular engineering and regeneration. It can be used in tissue vascularization, which is a core question in tissue engineering.⁵⁷ For example, intensive efforts have been made to fabricate vascularized tissue and organ models, such as the vascularized pancreas,^{58,59} adipose tissue,⁶⁰ bladder,⁶¹ islet,⁶² skin,⁶³ and so on. The model presented in this study can be further improved and applied in these *ex vivo* settings in the future. One critical aspect is perfusion, which is essential for the study of microvascular functions, including permeability,^{64,65} mechanobiology,⁶⁶ tumor cell and immune cell infiltration.⁶⁷ More advanced microvascular models can be made based on our method in combination with other engineering technologies, such as microfluidics,⁶⁶ electrospinning,⁶⁸ microspheres,⁶⁹ and 3D printing.⁵⁷

Conclusion

Our study established a method for expanding tubular microvessels on stiff substrates of regular culture dishes and retaining the ECs and pericytes from the same adult tissue. This model will hopefully provide more insights into the mechanisms of EC-pericyte interactions in tissue regeneration and diseases. The method established in this study also applies to other organs for engineering organ-specific microvascular models. As human microvessels can be relatively easily obtained from the subcutaneous soft connective tissues during minor surgeries, the platform presented in this study can hopefully be translated to clinical settings, benefiting the development of personalized microvascular engineering for precision medicine.

Acknowledgements

This work was supported by the Key Laboratory of Nucleic Acid Biology in Cardiovascular Disease, Shandong Province, and the International Research Centre for Non-coding RNAs and Translational Medicine, Qingdao. Thanks to Zhishang Chang, Qian Wen, Bing Wang, and Xuxia Song (the Laboratory of Biomedical Center, Qingdao University) for their technical help in confocal microscopy and flow cytometry.

Author contributions

DW designed the experiments. DW and JL wrote the manuscript. XS, YY, YL, YX, and DW performed primary cell isolation, cell culture, immunostaining and confocal microscopy. JM performed qRT-PCR. YL and LM performed flow cytometric analysis. ZW performed quantification of microvessels. HZ, XQ, PL, JL, and DW performed transcriptomic analysis.

Availability of data and materials

The data required to reproduce these findings can be made available upon reasonable request.

Declaration of conflicting interests

The author(s) declared no potential conflicts of interest with respect to the research, authorship, and/or publication of this article.


Ethical approval

The animal procedure was conducted according to the Ministry of Science and Technology guide for laboratory animal care and use and approved by the animal care and use committee of Qingdao University.

Funding

The author(s) disclosed receipt of the following financial support for the research, authorship, and/or publication of this article: This work was funded by the Natural Science Foundation of Shandong Province (No. ZR2019LZL001), National Nature Science Foundation of China (No. 32101020, 91849209, and 8187020984), and People's Livelihood Science and Technology Project of Qingdao (No. 20-3-4-41-nsh).

ORCID iD

Dong Wang  <https://orcid.org/0000-0003-3489-915X>

Supplemental material

Supplemental material for this article is available online.

References

- Eelen G, Treps L, Li X, et al. Basic and therapeutic aspects of angiogenesis updated. *Circ Res* 2020; 127: 310–329.
- Sweeney MD, Zhao Z, Montagne A, et al. Blood-brain barrier: from physiology to disease and back. *Physiol Rev* 2019; 99: 21–78.
- Nowak-Sliwinska P, Alitalo K, Allen E, et al. Consensus guidelines for the use and interpretation of angiogenesis assays. *Angiogenesis* 2018; 21: 425–532.
- Ligresti G, Nagao RJ, Xue J, et al. A novel three-dimensional human peritubular microvascular system. *Journal of the American Society of Nephrology : JASN* 2016; 27: 2370–2381.
- Lin NYC, Homan KA, Robinson SS, et al. Renal reabsorption in 3D vascularized proximal tubule models. *Proceedings of the National Academy of Sciences of the United States of America* 2019; 116: 5399–5404.
- Kemp SS, Aguera KN, Cha B, et al. Defining endothelial cell-derived factors that promote pericyte recruitment and capillary network assembly. *Arterioscler Thromb Vasc Biol* 2020; 40: 2632–2648.
- Wimmer RA, Leopoldi A, Aichinger M, et al. Human blood vessel organoids as a model of diabetic vasculopathy. *Nature* 2019; 565: 505–510.
- Aird WC. Phenotypic heterogeneity of the endothelium: I. Structure, function, and mechanisms. *Circ Res* 2007; 100: 158–173.
- Shen L, Song X, Xu Y, et al. Patterned vascularization in a directional ice-templated scaffold of decellularized matrix. *Eng Life Sci* 2021; 21: 683–692.
- Zheng Y, Chen J, Craven M, et al. In vitro microvessels for the study of angiogenesis and thrombosis. *Proc Natl Acad Sci U S A* 2012; 109: 9342–9347.
- Wang X, Phan DT, Sobrino A, et al. Engineering anastomosis between living capillary networks and endothelial cell-lined microfluidic channels. *Lab Chip* 2016; 16: 282–290.
- Ross SE, Hemati N, Longo KA, et al. Inhibition of adipogenesis by Wnt signaling. *Science* 2000; 289: 950–953.
- Piera-Velazquez S and Jimenez SA. Endothelial to mesenchymal transition: role in physiology and in the pathogenesis of human diseases. *Physiol Rev* 2019; 99: 1281–1324.
- Watanabe K, Ueno M, Kamiya D, et al. A ROCK inhibitor permits survival of dissociated human embryonic stem cells. *Nat Biotechnol* 2007; 25: 681–686.
- Kontos CD, Cha EH, York JD, et al. The endothelial receptor tyrosine kinase Tie1 activates phosphatidylinositol 3-kinase and Akt to inhibit apoptosis. *Cell Mol Biol* 2002; 22: 1704–1713.
- La Porta S, Roth L, Singhal M, et al. Endothelial Tie1-mediated angiogenesis and vascular abnormalization promote tumor progression and metastasis. *J Clin Investig* 2018; 128: 834–845.
- Goligorsky MS and Salven P. Concise review: endothelial stem and progenitor cells and their habitats. *Stem Cells Transl Med* 2013; 2: 499–504.
- Yao Y, Yao J and Boström KI. SOX transcription factors in endothelial differentiation and endothelial-mesenchymal transitions. *Front Cardiovasc Med* 2019; 6: 30.
- Tian X, Hu T, Zhang H, et al. Subepicardial endothelial cells invade the embryonic ventricle wall to form coronary arteries. *Cell Res* 2013; 23: 1075–1090.
- Tian X, Hu T, He L, et al. Peritruncal coronary endothelial cells contribute to proximal coronary artery stems and their aortic orifices in the mouse heart. *PLoS One* 2013; 8: e80857.
- Chen Q, Liu Y, Jeong HW, et al. Apelin(+) endothelial niche cells control hematopoiesis and mediate vascular regeneration after myeloablative injury. *Cell Stem Cell* 2019; 25: 768–783.e6.
- Masoud AG, Lin J, Azad AK, et al. Apelin directs endothelial cell differentiation and vascular repair following immune-mediated injury. *J Clin Investig* 2020; 130: 94–107.
- Deryugina EI and Quigley JP. Tumor angiogenesis: MMP-mediated induction of intravasation- and metastasis-sustaining neovasculature. *Matrix Biol* 2015; 44-46: 94–112.
- Felcht M, Luck R, Schering A, et al. Angiopoietin-2 differentially regulates angiogenesis through TIE2 and integrin signaling. *J Clin Investig* 2012; 122: 1991–2005.
- Olsen JJ, Pohl SÖ, Deshmukh A, et al. The role of Wnt signalling in angiogenesis. *Clin Biochem Rev* 2017; 38: 131–142.
- Pitulescu ME, Schmidt I, Giaimo BD, et al. Dll4 and Notch signalling couples sprouting angiogenesis and artery formation. *Nat Cell Biol* 2017; 19: 915–927.
- Limbourg FP, Takeshita K, Radtke F, et al. Essential role of endothelial Notch1 in angiogenesis. *Circulation* 2005; 111: 1826–1832.

28. Ramasamy SK, Kusumbe AP, Wang L, et al. Endothelial Notch activity promotes angiogenesis and osteogenesis in bone. *Nature* 2014; 507: 376–380.
29. Murad HAS, Rafeeq MM and Alqurashi TMA. Role and implications of the CXCL12/CXCR4/CXCR7 axis in atherosclerosis: still a debate. *Ann Med* 2021; 53: 1598–1612.
30. Song N, Huang Y, Shi H, et al. Overexpression of platelet-derived growth factor-BB increases tumor pericyte content via stromal-derived factor-1alpha/CXCR4 axis. *Cancer Res* 2009; 69: 6057–6064.
31. Deckelbaum RA, Lobov IB, Cheung E, et al. The potassium channel Kcne3 is a VEGFA-inducible gene selectively expressed by vascular endothelial tip cells. *Angiogenesis* 2020; 23: 179–192.
32. Rocha SF, Schiller M, Jing D, et al. Esm1 modulates endothelial tip cell behavior and vascular permeability by enhancing VEGF bioavailability. *Circ Res* 2014; 115: 581–590.
33. Annan DA, Maishi N, Soga T, et al. Carbonic anhydrase 2 (CAII) supports tumor blood endothelial cell survival under lactic acidosis in the tumor microenvironment. *Cell Commun Signal* 2019; 17: 169.
34. Rampon C, Prandini MH, Bouillot S, et al. Protocadherin 12 (VE-cadherin 2) is expressed in endothelial, trophoblast, and mesangial cells. *Exp Cell Res* 2005; 302: 48–60.
35. Mehta V, Pang KL, Rozbesky D, et al. The guidance receptor plexin D1 is a mechanosensor in endothelial cells. *Nature* 2020; 578: 290–295.
36. Armulik A, Abramsson A and Betsholtz C. Endothelial/pericyte interactions. *Circ Res* 2005; 97: 512–523.
37. Chen J, Luo Y, Hui H, et al. CD146 coordinates brain endothelial cell-pericyte communication for blood-brain barrier development. *Proc Natl Acad Sci U S A* 2017; 114: E7622–E31.
38. Owens GK, Kumar MS and Wamhoff BR. Molecular regulation of vascular smooth muscle cell differentiation in development and disease. *Physiol Rev* 2004; 84: 767–801.
39. James D, Nam HS, Seandel M, et al. Expansion and maintenance of human embryonic stem cell-derived endothelial cells by TGFbeta inhibition is Id1 dependent. *Nat Biotechnol* 2010; 28: 161–166.
40. Wang D, Wang A, Wu F, et al. Sox10(+) adult stem cells contribute to biomaterial encapsulation and microvascularization. *Sci Rep* 2017; 7: 40295.
41. Bianco P, Cao X, Frenette PS, et al. The meaning, the sense and the significance: translating the science of mesenchymal stem cells into medicine. *Nat Med* 2013; 19: 35–42.
42. Wang D, Li LK, Dai T, et al. Adult stem cells in vascular remodeling. *Theranostics* 2018; 8: 815–829.
43. Nalbach L, Müller D, Wrublewsky S, et al. Microvascular fragment spheroids: three-dimensional vascularization units for tissue engineering and regeneration. *J Tissue Eng* 2021; 12: 20417314211035593.
44. Frueh FS, Gassert L, Scheuer C, et al. Adipose tissue-derived microvascular fragments promote lymphangiogenesis in a murine lymphedema model. *J Tissue Eng* 2022; 13: 20417314221109957.
45. Laschke MW, Kontaxi E, Scheuer C, et al. Insulin-like growth factor 1 stimulates the angiogenic activity of adipose tissue-derived microvascular fragments. *J Tissue Eng* 2019; 10: 2041731419879837.
46. Später T, Worringer DM, Menger MM, et al. Systemic low-dose erythropoietin administration improves the vascularization of collagen-glycosaminoglycan matrices seeded with adipose tissue-derived microvascular fragments. *J Tissue Eng* 2021; 12: 20417314211000304.
47. Später T, Menger MM, Nickels RM, et al. Macrophages promote network formation and maturation of transplanted adipose tissue-derived microvascular fragments. *J Tissue Eng* 2020; 11: 2041731420911816.
48. Liguori I, Russo G, Curcio F, et al. Oxidative stress, aging, and diseases. *Clin Interv Aging* 2018; 13: 757–772.
49. Dejana E. The role of wnt signaling in physiological and pathological angiogenesis. *Circ Res* 2010; 107: 943–952.
50. Alexander MR and Owens GK. Epigenetic control of smooth muscle cell differentiation and phenotypic switching in vascular development and disease. *Annu Rev Physiol* 2012; 74: 13–40.
51. Yamazaki T, Nalbandian A, Uchida Y, et al. Tissue myeloid progenitors differentiate into pericytes through TGF-β signaling in developing skin vasculature. *Cell Rep* 2017; 18: 2991–3004.
52. Basile DP, Collett JA and Yoder MC. Endothelial colony-forming cells and pro-angiogenic cells: clarifying definitions and their potential role in mitigating acute kidney injury. *Acta Physiol* 2018; 222: e12914.
53. Okumura N, Nakano S, Kay EP, et al. Involvement of cyclin D and p27 in cell proliferation mediated by ROCK inhibitors Y-27632 and Y-39983 during corneal endothelium wound healing. *Investig Ophthalmol Vis Sci* 2014; 55: 318–329.
54. Kasai Y, Morino T, Mori E, et al. ROCK inhibitor combined with Ca(2+) controls the myosin II activation and optimizes human nasal epithelial cell sheets. *Sci Rep* 2020; 10: 16853.
55. Hirschi KK and D'Amore PA. Pericytes in the microvasculature. *Cardiovasc Res* 1996; 32: 687–698.
56. Ozerdem U and Stallcup WB. Pathological angiogenesis is reduced by targeting pericytes via the NG2 proteoglycan. *Angiogenesis* 2004; 7: 269–276.
57. Lee H, Jang T-S, Han G, et al. Freeform 3D printing of vascularized tissues: challenges and strategies. *J Tissue Eng* 2021; 12: 20417314211057236.
58. Magisson J, Sassi A, Xhema D, et al. Safety and function of a new pre-vascularized bioartificial pancreas in an allogeneic rat model. *J Tissue Eng* 2020; 11: 2041731420924818.
59. Han EX, Wang J, Kural M, et al. Development of a bioartificial vascular pancreas. *J Tissue Eng* 2021; 12: 20417314211027714.
60. Acosta FM, Stojkova K, Zhang J, et al. Engineering functional vascularized beige adipose tissue from microvascular fragments of models of healthy and type II diabetes conditions. *J Tissue Eng* 2022; 13: 20417314221109337.
61. Zhao F, Zhou L, Liu J, et al. Construction of a vascularized bladder with autologous adipose-derived stromal vascular fraction cells combined with bladder acellular matrix via tissue engineering. *J Tissue Eng* 2019; 10: 2041731419891256.
62. Song W, Chiu A, Wang LH, et al. Engineering transferrable microvascular meshes for subcutaneous islet transplantation. *Nat Commun* 2019; 10: 4602.
63. Baltazar T, Merola J, Catarino C, et al. Three dimensional bioprinting of a vascularized and perfusable skin graft using

- human keratinocytes, fibroblasts, pericytes, and endothelial cells. *Tissue Eng Part A* 2020; 26: 227–238.
64. Shen Z and He Y. Migration of a red blood cell in a permeable microvessel. *Med Nov Technol Device* 2019; 3: 100023.
 65. Rice O, Surian A and Chen Y. Modeling the blood-brain barrier for treatment of central nervous system (CNS) diseases. *J Tissue Eng* 2022; 13: 20417314221095997.
 66. Meng F, Cheng H, Qian J, et al. In vitro fluidic systems: Applying shear stress on endothelial cells. *Med Nov Technol Device* 2022; 15: 100143.
 67. Ozturk MS, Lee VK, Zou H, et al. High-resolution tomographic analysis of in vitro 3D glioblastoma tumor model under long-term drug treatment. *Sci Adv* 2020; 6: eaay7513.
 68. Liu Q, Ying G, Jiang N, et al. Three-dimensional silk fibroin microsphere-nanofiber scaffolds for vascular tissue engineering. *Med Nov Technol Device* 2021; 9: 100051.
 69. Wang P, Meng X, Wang R, et al. Biomaterial scaffolds made of chemically cross-linked gelatin microsphere aggregates (C-GMSs) promote vascularized bone regeneration. *Adv Healthc Mater* 2022; 11: e2102818.